Processing of hybrid laminates integrating ZrB2/SiC and SiC layers

AIMS Materials Science, 7(5): 552–564.
DOI: 10.3934/matersci.2020.5.552
Received: 04 May 2020
Accepted: 17 August 2020
Published: 24 August 2020

http://www.aimspress.com/journal/Materials

Research article

Processing of hybrid laminates integrating ZrB_2/SiC and SiC layers

Elisa Padovano[1,*], Francesco Trevisan[1], Sara Biamino[1,2] and Claudio Badini[1]

[1] Department of Applied Science and Technology, Politecnico di Torino, Torino, Italy
[2] National Interuniversity Consortium of Materials Science and Technology, Firenze, Italy

*** Correspondence:** Email: elisa.padovano@polito.it; Tel: +390110904708.

Abstract: Tape casting technique was used to develop hybrid laminates constituting by SiC and ZrB_2–SiC layers; the main aim is obtaining a structure which integrate the unique properties of these materials and potentially extent their application temperature range. Multilayer with ZrB_2–SiC layers stacked in between SiC ones were successfully processed. Thin cracks propagated in the composite layers without affecting SiC ones; their formation was due to residual stresses developed in the two materials because of the differences in their shrinkage and coefficients of thermal expansion. However, these cracks did not significantly affect the material properties: relative density, elastic modulus and flexural strength of hybrid laminates was indeed only slightly lower than those of laminates made up of layers with the same composition.

Keywords: tape casting; SiC; composites; hybrid structure; mechanical properties

1. Introduction

Silicon carbide is one of the most promising material for applications at high temperature in many fields such as gas turbine for power plants, fusion reactor walls and thermal protection systems thanks to its low density, excellent thermal and mechanical properties, at room as well as at high temperature [1–5]. One of the most interesting property of this material is its self-passivating behaviour in oxidizing environment. It is well known in fact, that SiC shows excellent oxidation resistance up to 1600 ℃ because of a thin silica passive layer forms on its surface [6]. Badini et al. [7] performed ground re-entry tests showing that a SiC laminate can survive 100 re-entry cycles up to a

maximum temperature of 1550 ℃, keeping almost completely the original mechanical features. However, at higher temperatures and under very low oxygen partial pressure this passive layer can be destroyed due to the occurring of active oxidation mechanism, which involves the formation of gaseous SiO and CO phases [6,8]. In addition, cristobalite melts at 1725 ℃ and then it evaporates. These factors, in addition to a low fracture toughness, limit the use of SiC for applications in severe environments such as those experienced by sharp profiles of space vehicles and hypersonic aircraft.

For very high temperature applications in severe conditions, ultra-high temperature ceramics (UHTCs) such as refractory carbides and borides of transition metals are considered the most promising candidates. These materials show rather good mechanical properties (such as strength and stiffness) combined with high melting temperatures, high resistance to environmental degradation and desired thermal properties [9–11]. In this context, ZrB_2 is considered as a promising candidate for aerospace applications due to its exceptional properties which include chemical inertness, one of the lowest density among UHTCs, and high electrical/thermal conductivities [12]. Nevertheless, its low oxidation resistance and low intrinsic sinterability are the main concerns for a wide application of these materials in severe environments.

The composite approach can partially overcome these limitations: previous studies proved the positive effects of adding SiC as secondary phase to ZrB_2. The addition of SiC can in fact promote the material densification, enhance its ablation resistance and moreover improve the mechanical performances [13,14]. However, the oxidation of ZrB_2 and ZrB_2–SiC composites results in the formation of a glassy phase, that easily volatilizes, and solid zirconia which melts well above 2000 ℃. Therefore ZrB_2-based ceramics could be used under extreme temperature conditions, but unfortunately their oxidation resistance is much worse than that of SiC below 1700 ℃ [15].

On the base of these considerations, there is not a single material which shows superior oxidation resistance all over a wide range of temperatures. The development of a hybrid material able to guarantee a good oxidation resistance while maintaining high mechanical performance could be effective for extending the temperature range for HTCs and UHTCs applications.

In this context, tape casting technology is a well-established technique for large-scale production of ceramic sheets and structures; thanks to its versatility and cost-effectiveness it is currently used in many application fields [16–20]. One of the main advantages associated to this production method is the possibility to fabricate ceramic laminates with a complex architecture, optimizing both the arrangement and the chemical composition of constituent layers. Moreover, laminates display improved toughness with respect to conventional ceramics thanks to the occurring of crack deflection mechanism and their resistance to the crack growth. This is caused by the weak interfacial bonds between the layers [21,22] and the residual stresses arising when layers with different composition are stacked [23–26].

To authors' knowledge, many papers are focused on the investigation of SiC or ZrB_2-based ceramics, but any investigations on hybrid structure integrating these two materials hasn't been published. In this paper, multilayer structures which includes ZrB_2–SiC layers stacked in between SiC ones were successfully prepared by tape casting technique and pressureless sintering. Their microstructures and mechanical behaviour have been investigated. A preliminary investigation of thermo-oxidative behaviour of laminates was also performed.

2. Materials and methods

Commercially available Zirconium Diboride (Grade B, H.C. Starck, with an average particle size of 2.25 μm) and α-SiC (H.C. Starck UF-15, with a mean particle size of 0.55 μm) were used as starting powders for the fabrication of the laminates. Carbon (Alfa Aesar flake 7–10 μm) and boron (H.C. Starck amorphous grade I, 1–2 μm) were used as sintering additives; they were added in a relative amount of 3wt% and 1 wt% respect to the SiC quantity.

ZrB_2 powders were milled for three hours in dry conditions using a tungsten carbide media to make their size comparable to that of SiC. Chamberlain et al. [27] reported that the reduction of ZrB_2 particles to sub-micrometer size enhances the material densification: the higher surface area of milled particles can in fact promote the driving force for sintering.

The composition of the layers to be stacked in between SiC ones was chosen on the base of a detailed study which investigates the effect of the relative amount of SiC and ZrB_2 phases on the properties of composite material [20]. Laminates made of ceramic sheets containing 80 vol% of ZrB_2 and 20 vol% of SiC show one of the best compromises in term of density and mechanical properties; therefore, this composition was used for the processing of composite interlayers of hybrid laminates; moreover, according to the literature this composition has been widely investigated for applications at high temperature [28–30].

The ceramic powders were dispersed in a mix of solvents (Ethanol ≥ 99.8% and Buthanol ≥ 99.4%, Sigma-Aldrich) and powders dispersant (Fish oil, Afom medical); then, they were mixed for 24 h in an alumina jar with alumina milling balls. Afterward, plasticizer (polyethylenglycole, Bisoflex 102 Cognis) and binder (polyvinilbutyral, Butvar B76 Solutia) were added into the previously prepared slurry and it was further mixed for 48 h. Tape casting was used for processing the sheets to be stacked in a multilayer structure; this technique allows in fact the production of laminates with complex architecture in terms of chemical composition, thickness, number and stacking position of the layers. The slurries were casted on a movable Mylar support with an advance speed of 100 mm/min and varying the height of doctor blade in order to obtain, after drying at room temperature, green ceramic sheets with tailored thickness. A doctor blade height of 1 mm resulted in green SiC sheets with a thickness of 240 μm (after drying). These operating conditions were adopted according to tape casting process developed in previous works [31,32]. Composite green layers with three different thicknesses were obtained by tuning the casting parameters: doctor blade heights of 1.0 mm (the same adopted for SiC tape), 0.7 mm, and 0.5 mm resulted in green ZrB_2/SiC sheets 190 μm, 140 μm, and 110 μm thick respectively. Tapes with rectangular shape were then stacked to obtain the so called "green" laminates.

They were submitted to a de-binding treatment up to 800 ℃ in an inert atmosphere in order to remove the organic components constituting the slurries; then they were sintered. Pressureless sintering was in fact performed (T.A.V. Cristalox oven) under argon atmosphere (99.99% purity, pressure around 550 mbar) at the temperature of 2200 ℃ maintained for 30 min.

Three kinds of specimens were obtained: multilayer containing 10 SiC sheets, samples constituted by ten ZrB_2/SiC composite layers and hybrid laminates made of 8 SiC layers plus 2 ZrB_2/SiC ones. Preliminary tests were performed in order to find the proper structure configuration: asymmetric structure suffered cracking and delamination; these problems can be avoided by

adopting a symmetric interposition of layers. Moreover, according to Sanchez-Herencia et al. [33], the presence of external layers in compression state, an improvement in strength can be achieved.

On the base of these considerations, hybrid structures were designed by stacking ceramic sheets according to the following symmetric structure: 3 SiC layers–1 ZrB_2/SiC layer–2 SiC layers–1 ZrB_2/SiC layer–3 SiC layers.

The thickness of sintered laminates was measured by using a Mitutoyo micrometer screw gauge (with a measuring range of 0–25 mm and a resolution of 0.01 mm). SiC and ZrB_2/SiC laminates show a thickness of 1.68 mm and 1.10 mm respectively after sintering; differently, the final thickness of hybrid laminates depends on the thickness of composite interlayers: ZS-1 and ZS-2 samples were prepared by using two ZrB_2/SiC green sheets 110 μm and 140 μm thick, which leads to obtain a thickness of respectively 1.53 mm and 1.56 mm for the sintered laminates. ZS-3 samples show a final thickness of 1.60 mm because of two composite green sheets with a thickness of 190 μm were used.

The thickness of layers with different composition was measured by analysing the optical images of polished cross sections of ceramic multilayers: the clear interface between SiC and composite layers makes possible the determination of the thickness of each interlayer. On the other hand, the thickness of a set of 2 or 3 SiC layers (it depends on the part of cross section that was considered) were measured; the average value of a single layer was calculated by dividing the total thickness of SiC layers by the number of considered layers. A minimum of 10 measurements were performed in order to check the reproducibility of the measured thickness for each kind of layer.

For each kind of laminate, 6 bars with length of 55 mm, width of 12 mm and thickness varying from 1.10 and 1.68 mm (on the base of different multilayer architecture under investigation) were processed according to the previously described processing path; a total of 30 samples were therefore produced and characterized.

The microstructure of the specimens was investigated using a scanning electron microscope (SEM-FEG Assing SUPRA 25, Zeiss, Germany equipped with EDS Oxford INCA X-Sight analyser) and an optical microscope (Leica DMI 5000 M, Leica Microsystem BV, Son, The Netherlands interfaced with Leica LAS software).

The bulk density of multilayers was measured through Archimede's method using water as the immersion medium. The mass of sintered samples was weighed using a balance with an accuracy of 1.0×10^{-5} g. The measurements were repeated on set of 6 samples for each multilayer structure in order to verify the reproducibility of obtained results. The density values were reported in a percentage value with respect to the theoretical density, which was calculated by the rule of mixtures.

The crystalline phases were identified using X-ray and micro-X ray diffractometer (Panalytical X'PERT PRO PW3040/60 and Rigaku D/Max Rapid with a 100 μm probe in size, both with Cu Kα radiation).

Elastic modulus was measured by the acoustic method which involves the analysis of transient natural vibration using RFDA MF basic instrument, IMCE, Belgium. Three-point bending tests were performed at room temperature adopting a 40 mm outer span and a crosshead speed of 0.1 mm/min (Sintech 10 D equipment, UNI EN 658.3 standard).

The oxidation resistance of laminates under investigation was preliminarily investigated by performing thermal gravimetric analyses (Mettler Toledo AG-TGA/STDA851e equipment). Samples

with size (3 × 3 × 1.10–1.68) mm^3 underwent two subsequent temperature runs which involved a heating step up to 1600 ℃ (heating rate of 10 ℃/min), and a cooling up to room temperature (heating rate of 18 ℃/min). This thermal cycle was repeated twice; all the tests were performed under oxidizing atmosphere (air flux of 50 mL/min).

3. Results and discussion

3.1. Microstructure

Figure 1a shows, as an example, the microstructure of polished cross-sections for ZS-2 laminate. The interfaces between the two materials are clearly distinguishable; the thickness of the composite layers is constant and uniform along the width of samples. EDS analyses confirmed that dark layers contained SiC, while grey ones were mainly constituted by ZrB_2.

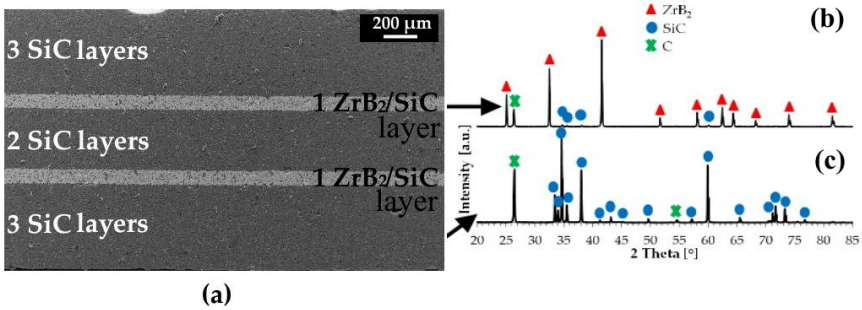

Figure 1. SEM image of multilayer polished cross section for ZS-2 sample (a); XRD patterns of the two materials constituent the multilayer (b) and (c).

The analysis of polished cross sections by using optical microscope allows to determine the thickness of SiC layers and composite ones. The following thicknesses were measured: SiC layers show a thickness of 163 ± 5 µm, while laminates fully constituted by composite layers reported ZrB_2–SiC layers with an average thickness of 105 ± 5 µm. The same thickness was determined for ZS-3 laminates (where thickest composite layers were used); on the other hand, a thickness of 63 ± 5 µm and 75 ± 5 µm was reported for composite layers constituting ZS-1 and ZS-2 laminates respectively (Table 1).

The thickness of the layers appreciably decreased during sintering. Sample cross section examination showed in fact that SiC layers shrank by 32%, while the shrinkage observed for ZrB_2–SiC layers is higher, in the range between 45% and 46%

Figure 1b,c show the XRD spectra obtained by analysing the layers with different compositions contained in the hybrid laminates: they confirm that no reaction occurred between the material components (SiC, ZrB_2, C and B) during the thermal treatments. No difference was observed with respect to the XRD spectra recorded for laminates fully constituted by identical layers only (made of SiC or ZrB_2/SiC composite). The only additional phase with respect to SiC and ZrB_2 ones was carbon, which gave a low intensity peak at 2-theta around 26.6 °. The carbon peak was due to

graphite flakes added as sintering aid, and to the residuals of degradation of the organic compounds occurring during de-binding treatment. EDS analyses confirmed the presence of the three previously reported phases, which can be clearly distinguished from Figure 2: SiC appears as dark grey area, while lighter grey areas correspond to ZrB_2. The presence of carbon particles in form of inclusions is evident in the polished cross section of hybrid samples ZS-1, ZS-2, and ZS-3 (Figure 2c–e) as irregular black spots. Few pores with size up to 12 μm were also observed; in correspondence of some of them some cracks appear within the composite layers. This outcome, in combination with the density measurements (Table 1), indicates that a rather good density degree was achieved for the laminates under investigation, although they were prepared without pressure assistance.

Table 1. Composition and relative density of laminates.

Laminates	Layer thickness after sintering (μm)	Relative density (% of the theoretical)
SiC	163 ± 5	95.2 ± 0.1
$80ZrB_2$–20SiC	105 ± 5	97.3 ± 0.2
ZS-1	SiC = 163; ZrB_2/SiC = 63	95.0 ± 1.5
ZS-2	SiC = 163; ZrB_2/SiC = 75	96.3 ± 1.8
ZS-3	SiC = 163; ZrB_2/SiC = 105	95.9 ± 1.0

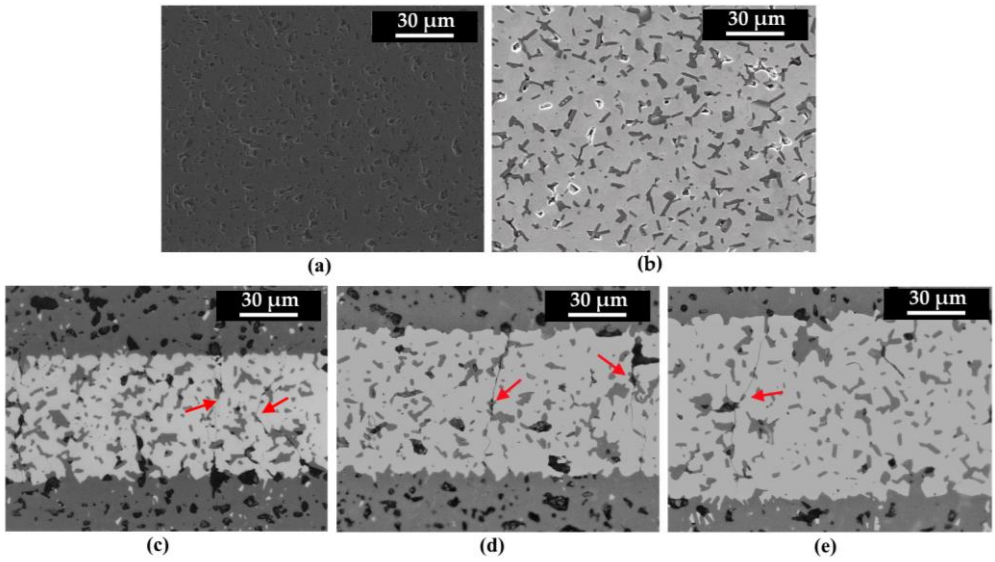

Figure 2. Polished cross sections of laminates: (a) made by 10 SiC layers, (b) made by 10 ZrB_2/SiC layers and integrating ZrB_2/SiC layers in between SiC ones (ZS-1 (c), ZS-2 (d), and ZS-3(e) samples).

Figures 2 compares the microstructure of laminates made of layers with same composition (10 SiC layers in Figure 2a and 10 ZrB_2/SiC composite layers in Figure 2b, respectively) with that of hybrid multilayer, putting in evidence the microstructure of composite interlayers (Figure 2c–e). A comparison of these micrographs shows the presence of some cracks in hybrid laminates; they propagate in the composite layers without appreciably affecting the neighbouring SiC ones. On the

contrary, these cracks were not observed in the microstructure of 100% SiC and 80% ZrB_2–20% SiC laminates.

These very thin cracks can be observed in the three kind of hybrid specimens, as shown in Figure 2c–e which are focused on the microstructure of interlayers. As previously discussed, the different colouring of phases constituting the interlayer allows to detect that the cracks originated within the composite layers, especially at the interfaces between SiC and ZrB_2 phases or between C and ZrB_2 particles (red arrows in Figure 2c–e). They propagated inside the ZrB_2 matrix in a twisted manner, moving preferentially towards carbon and SiC particles.

The presence of these cracks can be caused by the development of residual stresses within the laminates. As previously observed by many authors [34–39], multilayer structures which integrate different materials result in the development of residual stresses coming from both the processing methods and the different properties of the materials used for the fabrication of laminates.

Firstly, residual stresses can arise from the different sintering shrinkage occurring for SiC and composite layers. In fact, the shrinkage of composite layers was higher with respect to SiC ones, which resulted in tensile residual stresses inside the composite sheets. In addition, the formation of cracks can also be caused by residual stresses which developed during cooling from the sintering temperature. This is in agreement with the investigations reported by Hillman et al. [37] who fabricated laminates integrating thin ZrO_2 layers in between thicker layers made of Al_2O_3/ZrO_2. These authors found that pyrolysis of binder, densification and contraction during cooling from processing temperature induced the development of residuals stresses in multilayer structures.

In addition, development of residual stresses can be due to a mismatch of coefficient of thermal expansion (CTE) between the two materials placed into contact [38,39]. The processing of hybrid laminates involves the stacking of ceramics sheets made of SiC and ZrB_2-based composite, which show different CTE. In fact, the CTE of SiC is 5.1×10^{-6} ℃$^{-1}$ (25–1000 ℃) and 5.9×10^{-6} ℃$^{-1}$ (25–2500 ℃), while that of ZrB_2 is 5.9×10^{-6} ℃$^{-1}$ (25–1000 ℃) and 8.3×10^{-6} ℃$^{-1}$ (25–2500 ℃) [40,41]. The composite containing 80 vol% ZrB_2 and 20 vol% SiC has CTE values, calculated by the mixture rule, of 5.7×10^{-6} ℃$^{-1}$ (25–1000 ℃) and 7.8×10^{-6} ℃$^{-1}$ (25–2500 ℃) respectively. The ZrB_2/SiC composite shows higher CTE; as a consequence, its contraction during cooling from sintering temperature is higher with respect to that of silicon carbide. However, it is worth to note that the difference between CTEs of the two components in the lower temperature range involved during the de-binding treatment, is less important with respect to that occurring increasing the temperature up to the sintering one. Therefore, the significant mismatch between SiC and the composite thermal expansion coefficients causes thermal stresses at the interface between layers with different chemical composition. This results in compressive stresses within layers with lower CTE, that is silicon carbide layers, while tensile stresses develop within composite layers showing higher CTE.

The extent of the residual stresses depends on the composition of neighbouring layers, their properties (such as Young modulus and Poisson's ratio) and the thickness of each layer. The laminates under investigation were designed by stacking SiC flat elements alternating with composite ones. These elements had different thicknesses: SiC ones were made up of three stacked layers (or two in the case of the central SiC element only), while composite layer was constituted by a single sheet. For this kind of architecture the tensile residual stress sustained by the composite sheets can be evaluated according to the Eq 1 [42]:

$$\sigma_2 = \frac{n_2\, E_1\, E_2 h_1 (\alpha_2 - \alpha_1)\, \Delta T}{n_1\, (1-\nu_1) E_2\, h_2 + n_2 (1-\nu_2) E_1 h_1} \quad (1)$$

where 1 and 2 are the two laminate components (SiC and ZrB_2/SiC respectively), n_i is the number of i^{th} component, E_i and ν_i are the Elastic modulus (GPa) and Poisson's ratio of the i^{th} component, h_i is the thickness (mm) of the two kinds of layers, α_i their thermal expansion coefficient (K^{-1}) in the range from sintering to room temperature (ΔT).

On the base of Eq 1 the tensile stresses within the composite with lowest thickness (63 μm for ZS-1) is around 465 MPa; by increasing the interlayer thickness to 75 μm (ZS-2 sample) and 105 μm (ZS-3 sample) the entity of residual stresses only slightly decreased reaching values of 450 MPa and 430 MPa respectively. Because of these calculated values are higher with respect to the experimental determined flexural strength of the ZrB_2/SiC laminates (as shown in Table 2), the presence of cracks is not surprising. However, the stress entity did not lead to the failure of laminates during the processing.

3.2. Mechanical properties

Mechanical properties of hybrid laminates in term of elastic modulus and flexural strength are reported in Table 2; moreover, these properties are compared to those obtained for laminates made of layers showing all the same composition.

Table 2. Mechanical properties of SiC, ZrB_2/SiC and hybrid laminates.

Laminates	Elastic modulus (GPa)	Flexural strength (MPa)
SiC	339 ± 19	324 ± 24
80ZrB_2–20SiC	444 ± 10	277 ± 29
ZS-1	335 ± 15	322 ± 12
ZS-2	297 ± 14	313 ± 10
ZS-3	319 ± 22	289 ± 56

The elastic modulus of ZrB_2 is higher with respect to SiC one [20,43]; therefore, the stiffness of laminates constituted by 80% ZrB_2 + 20% SiC layers was observed to be higher than that of SiC multilayer. On the contrary, the flexural strength of laminates made of SiC sheets is higher with respect to that of the composite one 2.

The elastic modulus of ZS-1 hybrid laminate is similar to that of SiC laminate; by increasing the thickness of interlayer the elastic modulus is observed to slightly decrease. The presence of two not adjacent composite layers (which reported a higher elastic modulus with respect to SiC) in between SiC one seems not to improve the material stiffness. The flexural strength of hybrid laminates showed the same trend. Therefore, the presence of two composite interlayers, which show intrinsic lower flexural strength cause only a little decrease of flexural strength of the material.

On the base of these experimental results, hybrid laminates under investigation maintained good mechanical properties, which were found to be intermediate between those of multilayer constituting by 10 SiC layers and 10 ZrB_2/SiC layers. The mechanical behaviour improves by decreasing the

interlayer thickness. Therefore, the presence of micro cracks crossing the composite layers without affecting the SiC ones did not significantly affect the mechanical properties of the laminates.

Figures 3 shows the fracture surfaces of ZS-1 (Figure 3a), ZS-2 (Figure 3b), and ZS-3 (Figure 3c) laminates and puts in evidence the fracture mode of the hybrid materials. All the samples show a brittle fracture mode; however, some differences can be observed when SiC and ZrB_2/SiC layers are considered. In SiC layers the crack travels directly through the grains of the material and therefore cleavage planes, characteristic of transgranular fracture, can be observed. In the composite sheets a mixed fracture mode was observed: both intergranular (with crack propagation at the grain boundaries) and transgranular mechanisms were observed.

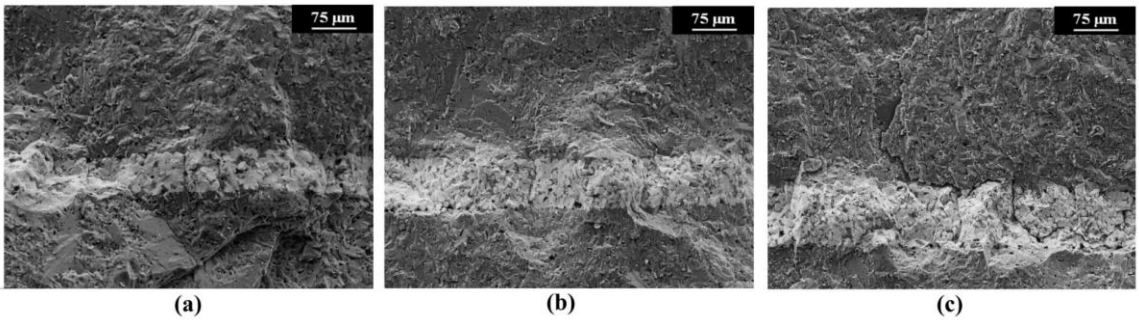

Figure 3. Fracture surface of ZS-1 (a), ZS-2 (b), and ZS-3 (c) samples.

Moreover, from Figure 3c there is evidence of crack deflection at the interfaces between SiC and ZrB_2 layers; the presence of layers with different composition can favourite an enhancement of the fracture work. The crack which nucleates in SiC layers did not travel right across the specimen thickness but was deflected at the interface between SiC and composite layers and then propagated parallel to this interface.

From the analysis of fracture surfaces there is no evidence that the presence of thin cracks within the composite interlayers can induce the fracture of samples.

3.3. Thermal gravimetric analyses

A preliminary investigation of thermo-oxidative behaviour of the laminates under investigation was performed. Figure 4a shows the TGA curves of SiC, ZrB_2/SiC and hybrid laminates collected up to 1600 ℃, while Figure 4b evidences more in details the behaviour of multilayer systems at temperature higher than 1000 ℃.

As expected, SiC laminates show a very small weight gain in the whole temperature range (continuous black curve in Figure 4b) due to the formation of a thin and continuous SiO_2 layers on the surface of the sample. This passive layer slows down the occurring of further oxidation [44], as evidenced by a weight increment lower than 0.2% observed during the second TGA run (dotted black curve in Figure 4b).

A very different trend is observed for laminates constituted by ZrB_2/SiC sheets: during the first run the samples weight slowly raises up to 1400 ℃; for higher temperature, the oxidation rate greatly

increases and reaches a mass gain of about 8.5% at 1600 ℃ (continuous blue curve in Figure 4a). Thanks to the presence of a significant amount of SiC, an oxide layer can grow on the laminates surface during this first heating run; this is confirmed by the lower weight gain observed during the second heating step (dotted blue curve in Figure 4b). This is in good agreement with the oxidation mechanism of ZrB_2/SiC composite widely studied in the literature [45–48].

The oxidation behaviour of hybrid laminates is similar to that of SiC multilayer: the presence of interlayers made of ZrB_2/SiC composite leads an increment of weight of about 1% and 0.6% after the first and second run respectively. These values are only slightly higher with respect to those observed for SiC laminates. As expected, the formation of passive layer during the first run can slow down the further oxidation of laminates, which results in a smaller weight gain after the second heating run with respect to the first one.

Moreover, the TGA curves for ZS-1, ZS-2, and ZS-3 samples (Figure 4, green, red and orange curves respectively) are very similar; the difference between the thickness of interlayers used for the fabrication of the two kinds of hybrid laminates is in fact very small.

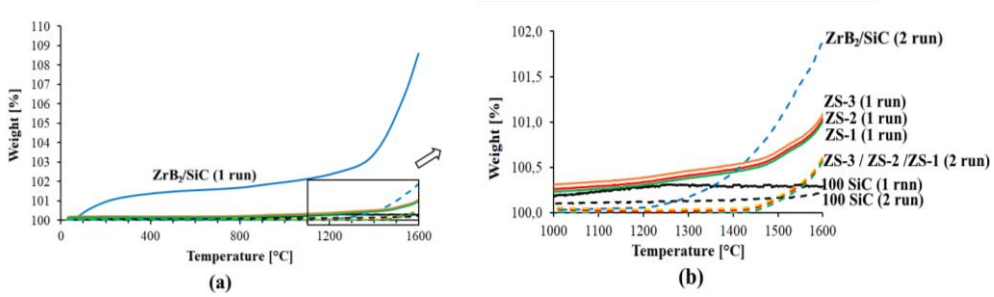

Figure 4. (a) Thermal gravimetric analyses of SiC (black curve), ZrB_2/SiC (Blue curve) and hybrid laminates (green curve for ZS-1, red curve for ZS-2, and red one for ZS-3) up to 1600 ℃. Continuous lines refer to first heating/cooling run, while dotted curves correspond to second run. (b) Focus on TGA curves at temperature higher than 1000 ℃ and weight increment up to 2%.

4. Conclusions

Laminates integrating ZrB_2/SiC layers in between SiC ones were successfully prepared by the tape casting technique and pressureless sintering. The integration of two materials with different properties was possible thanks to a preliminary milling of ZrB_2 starting powder which improved the material densification.

The micrographs of hybrid laminates showed the formation of thin cracks, which were not observed in SiC and ZrB_2/SiC structures. These cracks propagated in the composite layers, independently from their relative thickness with respect to SiC layers one. The presence of these cracks can be associated to different factors: the different sintering shrinkage of SiC and ZrB_2/SiC composite materials, the different contraction of these two materials which occurs during the cooling from sintering temperature, and the mismatch of coefficient of thermal expansion (CTE) between the two materials placed into contact.

The presence of these cracks weakly affected the mechanical properties of the hybrid laminates, which result only slightly lower with respect to those observed for multilayers made of layers with the same composition. The mechanical properties of hybrid laminates were in fact found to be intermediate between those of laminates made of SiC and ZrB_2/SiC layers.

A preliminary investigation of the thermo-oxidative behaviour was performed on hybrid laminates; their behaviour up to 1600 ℃ was observed to be similar to that of SiC laminates. In fact, the presence of ZrB_2/SiC layer in between SiC ones caused only a limited increase of mass gain up to 1600 ℃.

The obtained results for hybrid laminates show a slightly variation of both their mechanical and thermal properties with respect to those observed for SiC laminates. These promising results can justify a further investigation on these hybrid structures.

Conflict of interests

All authors declare no conflict of interest in this paper.

References

1. Takeuchi Y, Park C, Noborio K, et al. (2010) Heat transfer in SiC compact heat exchanger. *Fusion Eng Des* 85: 1266–1270.
2. Steen M, Ranzani L (2000) Potential of SiC as a heat exchanger material in combined cycle plant. *Ceram Int* 26: 849–854.
3. Casady JB, Johnson RW (1996) Status of silicon carbide (SiC) as a wide-bandgap semiconductor for high-temperature applications: A review. *Solid State Electron* 39: 1409–1422.
4. Joshi RP, Neudeck PG, Fazi C (2000) Analysis of the temperature dependent thermal conductivity of silicon carbide for high temperature applications. *J Appl Phys* 88: 265–269.
5. Pachaiyappan R, Gopinath R, Gopalakannan S (2015) Processing techniques of a silicon carbide heat exchanger and its capable properties—A review. *Appl Mech Mater* 787: 513–517.
6. Gulbransen EA, Jansson SA (1972) The high-temperature oxidation, reduction, and volatilization reactions of silicon and silicon carbide. *Oxid Met* 4: 181–201.
7. Badini C, Liedtke V, Euchberger G, et al. (2012) Self passivating behavior of multilayer SiC under simulated atmospheric re-entry conditions. *J Eur Ceram Soc* 32: 4435–4445.
8. Jacobson NS, Fox DS, Opila EJ (1998) High temperature oxidation of ceramic matrix composites. *Pure Appl Chem* 70: 493–500.
9. Squire TH, Marschall J (2010) Material property requirements for analysis and design of UHTC components in hypersonic applications. *J Eur Ceram Soc* 30: 2239–2251.
10. Levine SR, Opila EJ, Halbig MC, et al. (2002) Evaluation of ultra-high temperature ceramics foraeropropulsion use. *J Eur Ceram Soc* 22: 2757–2767.
11. Wuchina E, Opila E, Opeka M, et al. (2007) UHTCs: Ultra-high temperature ceramic materials for extreme environment applications. *Electrochem Soc Interface* 16: 30–36.

12. Neuman EW, Hilmas GE, Fahrenholtz WG (2013) Strength of zirconium diboride to 2300 ℃. *J Am Ceram Soc* 96: 47–50.
13. Hu P, Gui K, Yang Y, et al. (2013) Effect of SiC content on the ablation and oxidation behavior of ZrB_2-based ultra high temperature ceramic composites. *Materials* 6: 1730–1744.
14. Monteverde F, Bellosi A (2002) Effect of the addition of silicon nitride on sintering behaviour and microstructure of zirconium diboride. *Scripta Mater* 46 223–228.
15. Padovano E, Badini C, Celasco E, et al. (2015) Oxidation behavior of ZrB_2/SiC laminates: Effect of composition on microstructure and mechanical strength. *J Eur Ceram Soc* 35: 1699–1714.
16. Daudt NF, Hackemüller FJ, Bram M (2019) Manufacturing of Ti–10Nb based metal sheets by tape casting. *Mater Lett* 237: 161–164.
17. Muralidharan MN, Sunny EK, Dayas KR, et al. (2011) Optimization of process parameters for the production of Ni–Mn–Co–Fe based NTC chip thermistors through tape casting route. *J Alloys Compd* 509: 9363–9371.
18. Tietz F, Buchkremer HP, Stöver D (2002) Components manufacturing for solid oxide fuel cells. *Solid State Ionics* 152–153: 373–381.
19. Barcena J, Lagos M, Agote I, et al. (2013) SMARTEES FP_7 space project—towards a new TPS reusable concept for atmospheric eeentry from low earth orbit. *7th European Workshop on Thermal Protection System and Hot Structures*.
20. Padovano E, Badini C, Biamino S, et al. (2013) Pressureless sintering of ZrB_2–SiC composite laminates using boron and carbon as sintering aids. *Adv Appl Ceram* 112: 478–486.
21. Clegg WJ (1992) The fabrication and failure of laminar ceramic composites. *Acta Metall Et Mater* 40: 3085–3093.
22. Zhang J, Huang R, Gu H, et al. (2005) High toughness in laminated SiC ceramics from aqueous tape casting. *Scripta Mater* 52: 381–385.
23. Qin S, Jiang D, Zhang J, et al. (2003) Design, fabrication and properties of layered SiC/TiC ceramic with graded thermal residual stress. *J Eur Ceram Soc* 23: 1491–1497.
24. Prakash O, Sarkar P, Nicholson PS (1995) Crack deflection in ceramic/ceramic laminates with strong interfaces. *J Am Ceram Soc* 78: 1125–1127.
25. Lakshminarayanan R, Shetty DK, Cutler RA (1996) Toughening of layered ceramic composites with residua l surface compression. *J Am Ceram Soc* 79: 79–87.
26. Green DJ, Cai PZ, Messing GL (1999) Residual stresses in alumina–zirconia laminates. *J Eur Ceram Soc* 19: 2511–2517.
27. Chamberlain AL, Fahrenholtz WG, Hilmas GE (2006) Pressureless sintering of zirconium diboride. *J Am Ceram Soc* 89: 450–456.
28. Tripp WC, Graham HC (1971) Thermogravimetric study of the oxidation of ZrB_2 in the temperature range of 800 ℃ to 1500 ℃. *J Electrochem Soc* 118: 1195–1199.
29. Chamberlain A, Fahrenholtz W, Hilmas G, et al. (2004) High-strength zirconium diboride-based ceramics. *J Am Ceram Soc* 87: 1170–1172.
30. Zhang SC, Hilmas GE, Fahrenholtz WG (2008) Pressureless sintering of ZrB_2–SiC ceramics. *J Am Ceram Soc* 91: 26–32.

31. Biamino S, Antonini A, Eisenmenger-Sittner C, et al. (2010) Multilayer SiC for thermal protection system of space vehicles with decreased thermal conductivity through the thickness. *J Eur Ceram Soc* 30: 1833–1840.
32. Biamino S, Antonini A, Pavese M, et al. (2008) $MoSi_2$ laminate processed by tape casting: Microstructure and mechanical properties' investigation. *Intermetallics* 16: 758–768.
33. Sánchez-Herencia AJ, Baudín de la Lastra C (2009) Ceramic laminates with tailored residual stresses. *Bol Soc Esp Ceram* 48: 311–320.
34. Sglavo VM, Paternoster M, Bertoldi M (2005) Tailored residual stresses in high reliability alumina-mullite ceramic laminates. *J Am Ceram Soc* 88: 2826–2832.
35. Bermejo R, Pascual J, Lube T, et al. (2008) Optimal strength and toughness of Al_2O_3–ZrO_2 laminates designed with external or internal compressive layers. *J Eur Ceram Soc* 28: 1575–1583.
36. Thompson MJ, Fahrenholtz WG, Hilmas GE (2012) Elevated temperature thermal properties of ZrB_2 with carbon additions. *J Am Ceram Soc* 95: 1077–1085.
37. Hillman C, Suo Z, Lange FF (1996) Cracking of laminates subjected to biaxial tensile stresses. *J Am Ceram Soc* 79: 2127–2133.
38. Spowart JE, Dève HE (2000) Compressive failure of metal matrix composites, In: Kelly A, Zweben C, *Comprehensive Composite Materials*, Elsevier, 3: 221–245.
39. Mari D, Krawitz AD, Richardson JW, et al. (1996) Residual stress in WC-Co measured by neutron diffraction. *Mater Sci Eng A-Struct* 209: 197–205.
40. Shackelford JF, Alexander W (2001) *CRC Materials Science and Engineering Handbook*, 4 Eds., New York: CRC press, 49: 1557–1558.
41. Bansal PN (2006) *Handbook of Ceramic Composites*, Springer Science & Business Media, 200.
42. Zhang X, Zhou P, Hu P, et al. (2011) Toughening of laminated ZrB_2–SiC ceramics with residual surface compression. *J Eur Ceram Soc* 31: 2415–2423.
43. Guo SQ (2009) Densification of ZrB_2-based composites and their mechanical and physical properties: A review. *J Eur Ceram Soc* 29: 995–1011.
44. Jacobson NS, Myers DL (2011) Active oxidation of SiC. *Oxid Met* 75: 1–25.
45. Niu Y, Wang H, Li H, et al. (2013) Dense ZrB_2–$MoSi_2$ composite coating fabricated by low pressure plasma spray (LPPS). *Ceram Int* 39: 9773–9777.
46. Monteverde F, Savino R (2007) Stability of ultra-high-temperature ZrB_2–SiC ceramics under simulated atmospheric re-entry conditions. *J Eur Ceram Soc* 27: 4797–4805.
47. Karlsdottir SN, Halloran JW, Henderson CE (2007) Convection patterns in liquid oxide films on ZrB_2–SiC composites oxidized at a high temperature. *J Am Ceram Soc* 90: 2863–2867.
48. Fahrenholtz WG (2007) Thermodynamic analysis of ZrB_2-SiC oxidation: Formation of a SiC-depleted region. *J Am Ceram Soc* 90: 143–148.